



Micellization thermodynamics as a function of the temperature of a cationic zwitterionic dodecyl phosphocholine and anionic sodium dodecyl sulfate mixed micelles with fluorometry

Raghda Abo Gabal¹ · Sabreen Osama² · Nemany Hanafy³ · Ahmed Oraby²

Received: 2 August 2022 / Accepted: 8 February 2023 / Published online: 19 February 2023
© The Author(s) 2023

Abstract

As fluorescence parameters such as lifetime, quantum yield, anisotropy and polarisation quantum are extremely sensitive to fluorophores' microenvironmental changes, changes in the properties of the fluorescence probe have been widely used to study hydrophobic interactions in protein and membrane biology. The current study determines the critical micelle concentration (CMC) of mixed micelles of sodium dodecyl sulfate (SDS) and cationic surfactant N-dodecyl phosphocholine (DPC) based on fluorescence intensity measurements. biomolecular structure analysis and dynamics revealed through the measure of changes in the nanosecond time range. As the temperature rises, the onset of micellization tends to occur at higher concentrations. It was measured versus micelle concentration over a temperature range of (288–338) K. The obtained results were used to estimate the micellization thermodynamic parameters. Surfactant CMC drops to a minimum ($T = 308$ K) and then rises with temperature forming a parabolic curve as a function of temperature, according to experimental data. The CMCs are first correlated by a polynomial equation to determine the enthalpy of micellization. Both ΔH_{mic} and ΔS_{mic} appear to decrease monotonically as temperature rises. ΔG_{mic} is negative, indicating that the micellization process is exothermic and favorable. The compensation temperature (T_c) ranged from (313–318) K by linear regression over the whole temperature range and for DPC, SDS, and mixed micelles together.

Keywords CMC · Micelle micellization thermodynamic · Ionic surfactant · Pyrene · SDS · DPC · Fluorometric intensity

1 Introduction

Some factors influence the success of a synthetic therapeutic carrier [1]. First, the drug's physiochemical limitations must be addressed; second, the biological barriers to reaching the targeted tumorous tissue must be addressed. Concerning each disease's distinct characteristics (the plasma

and subsequent protein corona), recommend the development of personalized nanomedicine[2]. Nanocarriers are being developed for a variety of malignancies, as well as chemotherapy medications [3]. The ability of membrane-active peptides to associate with the cell membrane is closely related to their structure and activity[4]. Among the most notable membrane models suited for membrane interaction investigations, the match of biological membranes diminishes in the sequence of liposomes, micelles, and mixed micelles [5]. Because of their short rotational correlation time, micelles represent a reasonable compromise between an appropriate membrane model and the need for a somewhat quick tumbling mechanism. Specifically, several micellar carriers with hydrophobic chemotherapy drugs in their core are making great progress in clinical trials[6]. Surfactants aqueous solutions such as dodecyl phosphocholine (DPC) and sodium dodecyl sulfate (SDS) are the most often used micellar membrane-mimicking systems. DPC forms micelles that have a zwitterionic surface that closely resembles vertebrate cell membranes. DPC/SDS form a membrane

✉ Raghda Abo Gabal
raghdaabogabal@gmail.com

Ahmed Oraby
ahoraby@yahoo.com

¹ Mansoura University Urology and Nephrology Center, Mansoura, Egypt

² Department of Physics, Faculty of Science, Mansoura University, Mansoura 3551, Egypt

³ Nanomedicine Group, Institute of Nanoscience and Nanotechnology, Kafrelsheikh University, Kafr El Sheikh 33516, Egypt

with a minor dominance of negative charges, as observed in DPC/SDS mixed micelles, which can also be utilized to imitate the electrostatic characteristics of vertebrate plasma. However, using SDS to simulate a membrane environment is not always a good idea. The addition of SDS to DPC, on the other hand, can be explained by the increased stability of the zwitterionic micelles and the enhancement of these solute–solute interactions [7].

In an aqueous solution, the hydrophilic portion of the amphiphilic solvates the micelle structure to minimize unfavorable interactions between the polar solvent and the hydrophobic region. Micelles have proven useful in medical applications due to their ability as hydrophobic guest molecules are captured. Micelle assembly must be well-characterized before it can be used in medical applications. Micelle assembly is a concentration-dependent process with a distinct transition at the critical micelle concentration (CMC), suggesting enhancement of the hydrophobic microenvironments monitored by both drugs in the pre-micellar and self-aggregates. Surfactant molecules can be free in solution at concentrations lower than this. As the surfactant concentration rises above the critical micelle concentration, the molecules congregate forming micelles. While the CMC is largely determined by the surfactant's chemical properties, it is also affected by surrounding environmental factors like pH, temperature, and ionic strength. Several techniques, including electric conductivity, light scattering, surface tension, and viscosity, have been employed to detect the CMC of various surfactants [8]. Unlike surface tension and conductivity methods, which require indirect determination, utilizing the fluorescence probes to determine the point at which micelles first form allows direct determination. Besides, that surface tension and conductivity methods measure the surface concentration of surface active species and the monomer's electrolyte activity, not the micelle's presence in the solution [9]. Fluorescence is the phenomenon displayed when a substance transitions from the electronically excited state to the ground state. However, the association may occur between excited-state molecules and ground-state molecules, thereby causing an emission (fluorescence). This state is referred to as an exciting complex. If it comprises identical molecules, it is referred to as an excited dimer (excimer). If it comprises two different molecules, it is referred to as an exciplex [10]. Pyrene is one of the well-investigated molecules for excimer-based sensing, with a monomer emission at around 370–380 nm and an excimer emission at 460–480 nm [11]. Pyrene partitions itself between the aqueous and hydrocarbon-like micellar core. It is a spatially fluorescent probe for CMC determination using the F3/F1 method, which is the ratio between the first and third vibronic peaks at 374 nm and 483 nm, respectively as excitation develops at 336 nm [12, 13]. Monomeric fluorescence displays an ensemble of emission peaks (375–405 nm) and an additional band (called

excimer) at ~460 nm when two fluorophores are spatially proximal. An intense excimer band was revealed when the distance between pyrenes was ~5 Å from each other [14]. The emitted fluorescence spectrum is detected using a fluorometer, which requires a quartz cuvette, and is then analyzed for CMC determination. It has been discovered that I_1/I_3 for pyrene is highly dependent on the surfactant head group, but is unaffected by surfactant concentration, hydrocarbon chain length, or the presence of external additives such as hexane or electrolytes [15]. Li investigated the factors affecting CMC determination with pyrene as a probe [16]. Akbas referred to the chief role of thermodynamic parameters to accomplish the monomer-micelle equilibrium with solvent [17]. The determination of micellization thermodynamic parameters in an aqueous environment, such as the Gibbs free energy G_{mic} , enthalpy ΔH_{mic} , entropy ΔS_{mic} , Heat capacity ΔC , and Enthalpy–entropy compensation is more significant since these factors evaluate the relative relevance of hydrophobic interactions, surfactant-water contact, and head-group repulsion (for ionic surfactants). The temperature dependence of the critical micelle concentration can be used to calculate these parameters CMC. sikorska have used isothermal titration calorimetry to study the thermodynamic properties of micellization for DPC, SDS and their mixtures [7]. In this work the thermodynamics and the micelle formation of DPC, SDS, and DPC/SDS mixed systems versus temperature, pyrene is used as a hydrophobic fluorescent probe to determine the formation of micellar structures. The fluorometric analysis of binary mixtures of sodium dodecyl sulfate (SDS) and the cationic surfactant N-dodecyl phosphocholine (DPC) is presented in this study.

2 Materials and methods

2.1 Materials

The cationic surfactant N-dodecyl phosphocholine (DPC) was supplied by Sigma-Aldrich Co, USA, Mol Weight: 283.5 g/mol (850336P), Sodium dodecyl sulfate (SDS) was provided by the Sigma Aldrich Co, USA Mol Weight: 288.38 g/mol (85F-0414), Pyrene was purchased from Chem-lab NV, Belgium, Mol Weight: 202.26 g/mol (CL00.168.0025), distilled water (DW).

2.2 Preparation of solutions

2.2.1 N-dodecyl phosphocholine solution preparation

A stock solution of DPC with a concentration of 0.05 mol/L, (0.44 g in 25 mL of DW), was stirred magnetically overnight before use.

2.2.2 Sodium dodecyl sulfate solution preparation

A stock solution of SDS with a concentration of 0.04 mol/L, (0.34 g of SDS in 25 mL of DW), stirred magnetically overnight before the use.

2.2.3 Pyrene chloroform stock solution preparation (0.5 mM)

Preparing 6.0×10^{-7} mg/mL of pyrene in water, about 10.1 mg of pyrene ($M_r = 202.3$) added to 80 mL of chloroform into a 100 mL volumetric flask, which is slightly lower than the saturation solubility, magnetically stirred for dissolution, the solution rotary vaporized then the flask filled to the mark with distilled water.

2.3 Preparation of samples

A concentrated surfactant solution (2CMC) that is diluted a ten-fold serial dilution, the concentrated surfactant solution containing a specified amount of pyrene (1.0–2.0 μ M) was then poured to separate into 5 mL volumetric flasks, which were then filled with water to the mark [16].

2.4 CMC Determination using pyrene as a fluorescent dye

The critical micelle concentration (CMC) was determined by using fluorescent pyrene, ultra-sonication samples for 30 min, and measuring fluorescence after 6 h of equilibrium at 25 °C with a fluorometric (Denovix-QFX) Fig. 1 using 2.5 mL in quartz vials. The excitation wavelength was 336 nm, and the emission spectrum was 350–450 nm. The excitation spectra of pyrene from 350 to 900 nm were set at 336 nm for different dilutions assessed using a spectrofluorometer (Jasco FP-6500, Japan) and two-photon laser confocal microscopy (690–1040 nm) (Xenon arc Lamp 150 W). The intensity of the fluorescence was plotted against

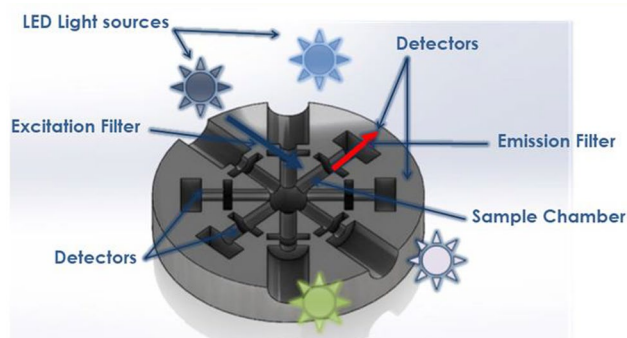


Fig. 1 Schematic diagram of the Fluorometer apparatus (Denovix-QFX)

surfactant concentration, and the point at which these lines intersected was calculated and determined to be the CMC. The fluorescence lifetime and anisotropy have been measured based on a time-resolved spectrofluorometer from Edinburgh Company, England model FS5. The light source used was a picosecond pulsed laser with a wavelength of 452 nm. The laser power has been optimized to the highest molecular brightness. All measurements have been corrected by the instrument response function of the apparatus.

2.5 Fourier Transform Infrared Spectroscopy (FTIR)

FTIR spectra are analyzed with an FTIR spectrophotometer (PerkinElmer-99075, German) using the ATR-IR technique in the spectral range 4000–450 cm^{-1} . Fourier transform infrared (FTIR) spectroscopy is an analytical technique used to identify the surface chemical structure (functional group, bonding types) [18]. Samples were freeze-dried under vacuum before measurements.

3 Results and discussion

3.1 CMC determination

The vibronic structure of the pyrene emission spectrum is polarity-dependent. The allowed and strong band F_3 at 384 nm exhibits minimal intensity variations with solvent polarity, in contrast to the forbidden peak F_1 at 373 nm, the intensity of which is strongly polarity-dependent. As a result, changes in the intensity ratio of F_3 and F_1 represent the fluctuations in the pyrene microenvironment and could be used to calculate the surfactants CMC. Pyrene senses the polar environment of water molecules in the absence of surfactant, resulting in an F_3/F_1 ratio greater than when the CMC is reached (the surroundings of pyrene becomes progressively less polar as reflected by a reduction of the F_3/F_1 ratio) [19, 20]. We plot the fluorescence intensities of surfactant concentration for a DPC, b 5:1 DPC/SDS, c 3:1 DPC/SDS, d 1:1 DPC/SDS, and e SDS to determine the critical micelle concentration of cationic and anionic surfactants [21]. Certainly, many important properties of surfactants in solutions change dramatically at this concentration CMC value. Figure 2 depicts the F_3/F_1 variations of the surfactants versus concentration and temperature. Breaks in the F_3/F_1 according to surfactant concentration curves are visible in this figure for all temperatures; these breaks are due to the micelle formation. At low concentrations of surfactant, there is little cooperation with the probe characteristic of a polar environment sensed by the probe. This is followed by a binding region within which there is a large uptake of surfactant with the possibility of the formation of surfactant pre-micellar aggregates, which effectively incorporate the probe.

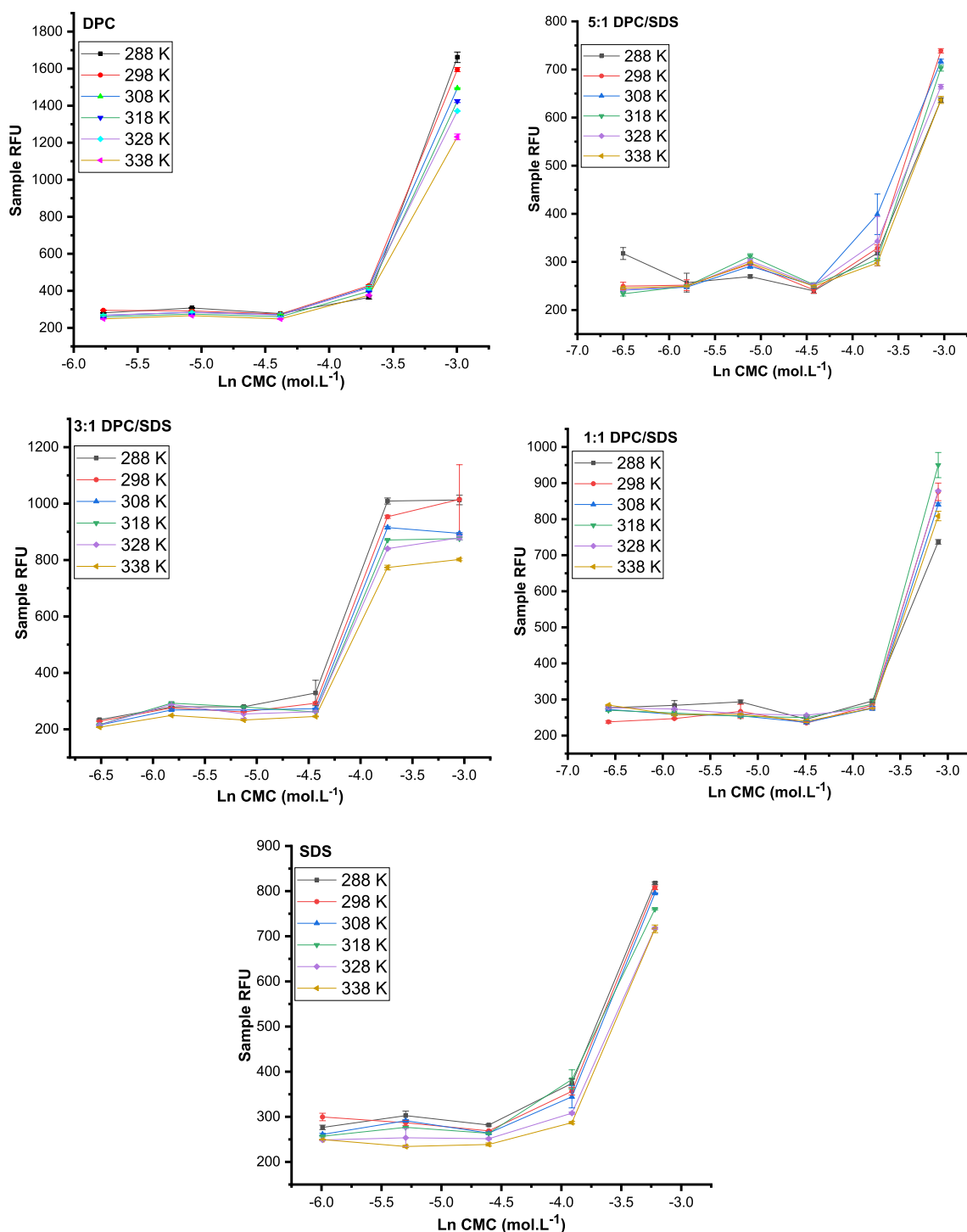


Fig. 2 Variation of CMC as a function of surfactant concentration for **a** DPC, **b** 5:1, **c** DPC/SDS, **d** 3:1 DPC/SDS, **e** 1:1 DPC/SDS, and **f** SDS as a function of temperature mixed micelles system in water at different temperatures

As extra surfactant is added, a CMC is reached which will be identified from the binding isotherm as a simultaneous rapid increase within the vibronic ratio and therefore the free surfactant concentration in solution becoming constant characteristic of a more hydrophobic intracellular environment

sensed with the aid of using the probe. Figure 1. shows the presence of two extrema indicating two CMC values denoted by CMC₁ and CMC₂ for 5:1 DPC/SDS and 3:1 DPC/SDS. The CMC value of pure DPC at 298 K is 0.0245 M. The CMC was calculated for each temperature by intersecting the

Table 1 CMC and ln CMC as a function of temperature

Micelles	T(k)	CMC (mol L ⁻¹)	Ln CMC (mol L ⁻¹)
DPC	288	0.0251 ± 0.01	-3.6849 ± 0.38
	298	0.0245 ± 0.00	-3.7091 ± 0.01
	308	0.0245 ± 0.00	-3.7091 ± 0.01
	318	0.0248 ± 0.00	-3.6969 ± 0.01
	328	0.025 ± 0.00	-3.6889 ± 0.01
	338	0.0251 ± 0.00	-3.6849 ± 0.01
5:1 DPC/SDS	288	0.0244 ± 0.00	-3.7132 ± 0.01
	298	0.0209 ± 0.00	-3.8680 ± 0.01
	308	0.0195 ± 0.00	-3.9373 ± 0.02
	318	0.0219 ± 0.00	-3.8213 ± 0.00
	328	0.0224 ± 0.00	-3.7987 ± 0.07
	338	0.0245 ± 0.00	-3.7091 ± 0.01
3:1 DPC/SDS	288	0.012 ± 0.00	-4.4229 ± 0.03
	298	0.0112 ± 0.00	-4.4918 ± 0.02
	308	0.011 ± 0.00	-4.5099 ± 0.01
	318	0.0123 ± 0.00	-4.3982 ± 0.01
	328	0.0126 ± 0.00	-4.3741 ± 0.01
	338	0.0126 ± 0.00	-4.3741 ± 0.01
1:1 DPC/SDS	288	0.0251 ± 0.00	-3.6849 ± 0.01
	298	0.0219 ± 0.00	-3.8213 ± 0.01
	308	0.0209 ± 0.00	-3.8680 ± 0.01
	318	0.0224 ± 0.00	-3.7987 ± 0.01
	328	0.0239 ± 0.00	-3.7339 ± 0.00
	338	0.0245 ± 0.00	-3.7091 ± 0.00
SDS	288	0.0178 ± 0.00	-4.0286 ± 0.01
	298	0.0169 ± 0.00	-4.0804 ± 0.08
	308	0.0182 ± 0.00	-4.0063 ± 0.01
	318	0.0195 ± 0.00	-3.9373 ± 0.02
	328	0.0199 ± 0.00	-3.9170 ± 0.01
	338	0.0204 ± 0.00	-3.8922 ± 0.00

two slopes of each curve. Table 1 displays CMC values and ln CMC. The CMC of SDS at 298 K is 0.0169 M. Addition of SDS to the DPC micelle results in a decrease in the CMC values to 0.0209, 0.0112, and 0.0219 M at 298 K for the 5:1 DPC/SDS, 3:1 DPC/SDS, and 1:1 DPC/SDS systems. At 298 K. While the minimum CMC for 5:1 DPC/SDS, 3:1 DPC/SDS, and 1:1 DPC/SDS micelles occurs at 308 K. However, it is very close to that obtained for pure DPC at 308. For the 5:1 DPC/SDS, and 3:1 DPC/SDS, the second transition region at CMC₂ is much broader, the CMC₂ decreases with increasing temperature and decreasing DPC concentration. At low temperatures, both steps of the micelle formation processes in mixed micelles occur in two phases. Micellization occurs as a single step at higher temperatures, with only one CMC. As the probability of hydrogen bond formation lowered at elevated temperatures, so at the first the CMC lowers and then raises. As previously stated, the CMC for the binary system (3:1 DPC/SDS) with surfactants with

different charges will be significantly lower than that of each surfactant because of electrostatic attraction [22]. Because of electrostatic attractions between the cationic function group of DPC and the anion of SDS, it is assumed that the interaction of zwitterionic DPC and anionic SDS is beneficial [23]. In this work, CMC values were estimated by the fluorimeter using pyrene as a probe molecule, which has also displayed to be sensitive to obtain corrupted values. Figure 3 displays a spectral comparison of pyrene diluted in aqueous solutions with a varied concentration of representative DPC, 3:1 DPC/SDS, and SDS. The increase in Fluorescence intensity with the increase in surfactant concentration is because of the integration of solute molecules to micelles. As more pyrene molecules are incorporated to micelles core the absorbance value. Besides the obvious increase in fluorescence intensity, whilst the concentration increases, a red shift of the maxima is likewise perceived. As the hydrophobic probe (pyrene) pass into the micelles hydrophobic core from the external aqueous medium.

Using time-resolved fluorescence and steady-state anisotropy techniques, Fig. 4 showed the fluorescence spectra of Pyrene as a free dye and Pyrene with 3:1 DPC/SDS in aqueous solution for 3:1 DPC/SDS surfactant (0.012 Mol/L) and (0.0056 Mol/L). Pyrene in water solution, the emission spectrum has only less broadband with a maximum at 524 nm on excitation with 452 nm pulsed laser), the broadening could be a result of such similar spacing in the vibrational bands of both excitation and ground state bands. On inseting a small amount of 3:1 DPC/SDS (0.012 Mol/L) in pyrene, the fluorescence intensity red-shifted to 532 nm with the appearance of an extra well-defined sharp band fluorescence band around 380 nm. The shift proves the chemical reaction between the micelles and the dye which is also clear from the changing of the energy gap. Moreover, the new hybrid energy levels seem to disorder the vibrational levels spacing [24] and make it different than those of the ground state causing decreasing in the emission band broadening. The previous emission spectra prove the integration of the Pyrene to the micelles, To confirm that the Pyrene was inserted into the micelle molecules. In this regime, different techniques could be utilized such as fluorescence (Cross) Correlation Spectroscopy (FCS, FCCS) and even Förster resonance energy transfer (FRET). One of the methods which could be proven is the time decay anisotropy, by fitting the anisotropy decay curve one could obtain the correlation time. Time-resolved fluorescence anisotropy measurement is used as an indirect method to determine the structural arrangements [25]. The rotational correlation time (tc) of a probe molecule in micellar assembly is determined using time-resolved anisotropy measurements, which is considered evidence of the diffusing molecule size and shape being approximately the same. Using the Einstein-Stokes

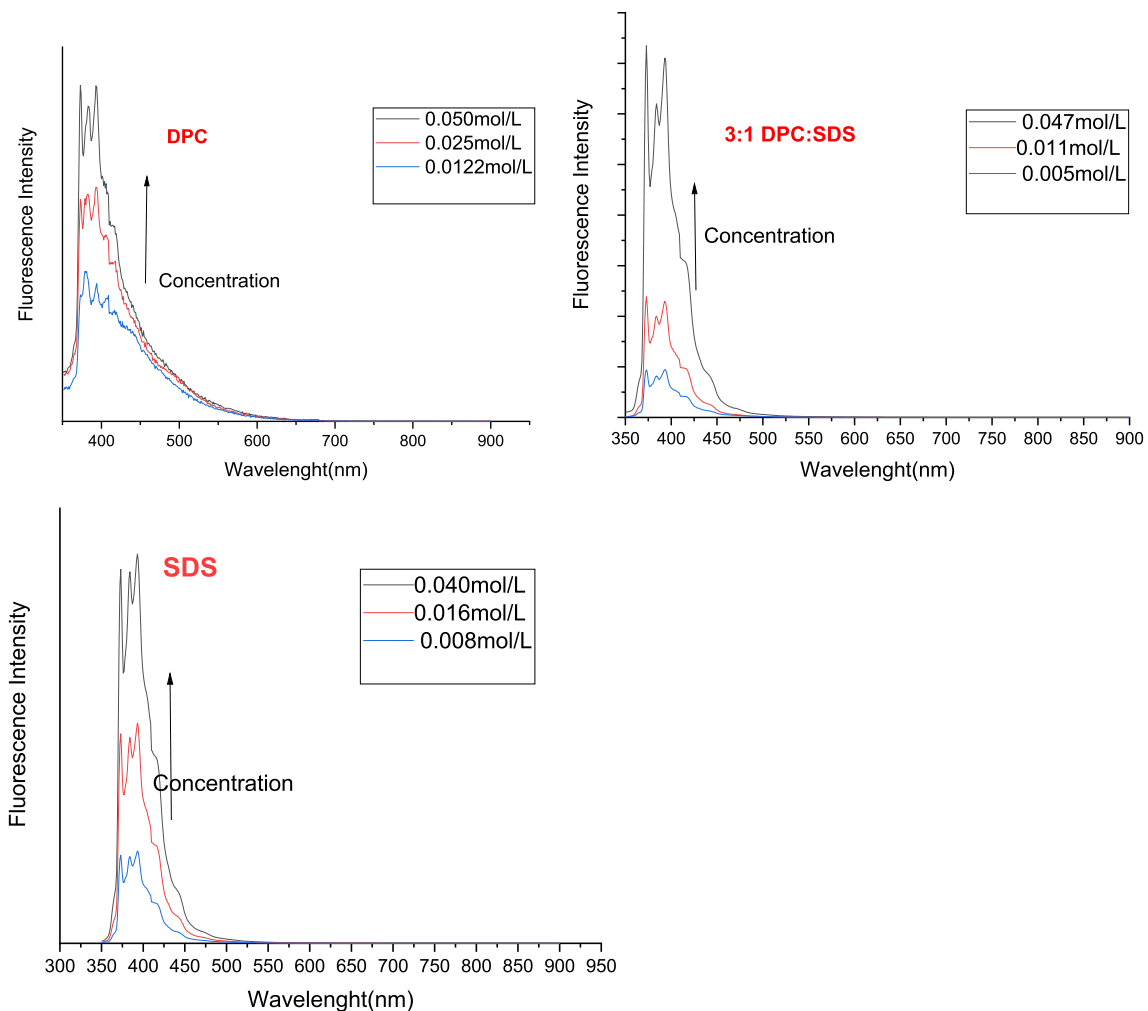


Fig. 3 Fluorescence spectra of Pyrene at various concentrations of a DPC, 3:1 DPC/SDS, and SDS

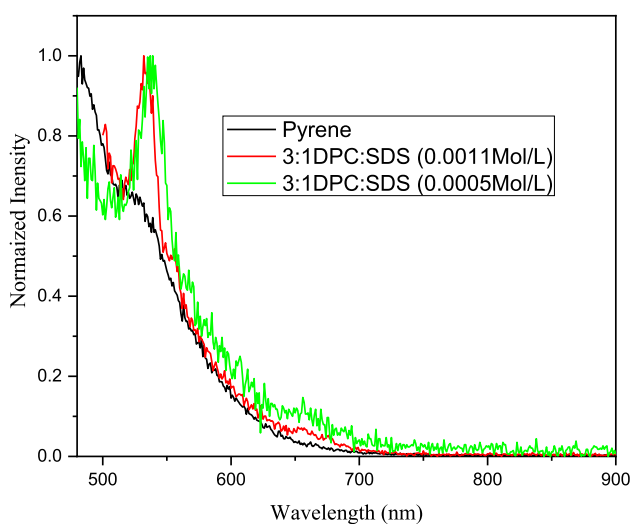


Fig. 4 Fluorescence spectrum of pyrene dye (black line), 3:1 DPC:SDS (0.01 Mol/L) (red line) and DPC: SDS 3:1(0.056 Mol/L) (green line), excited with 452 nm pulsed laser

Table 2 Fitting parameters of the time decay anisotropy

Sample	r_0	r_∞	τ_c (ns)	$V \times 10^{30}(\text{m}^3)$
1:3 DPC: SDS (0.011 Mol/L)	0.4	0.102	0.696	2.86
1:3 DPC: SDS (0.011 Mol/L)	0.6	0.18	0.682	2.8

relation one could estimate the hydrodynamic radius of the diffused molecule. the fitting parameters are presented in Table 2. Figure 5 shows the time decay anisotropy decay of 3:1 DPC/SDS surfactant (0.012 Mol/L) and (0.0056 Mol/L) fits the tail fitting exponential decay function with a rotational time of 0.696, 0.682 ns, obviously indicating similar structural arrangements[26]. The increase of anisotropy accompanied with a decrease of the mobility because of the monomer-micelle equilibrium (5–12 mM surfactant). From the rotational correlation time, one could use the following relation to calculate the hydrodynamic molecular

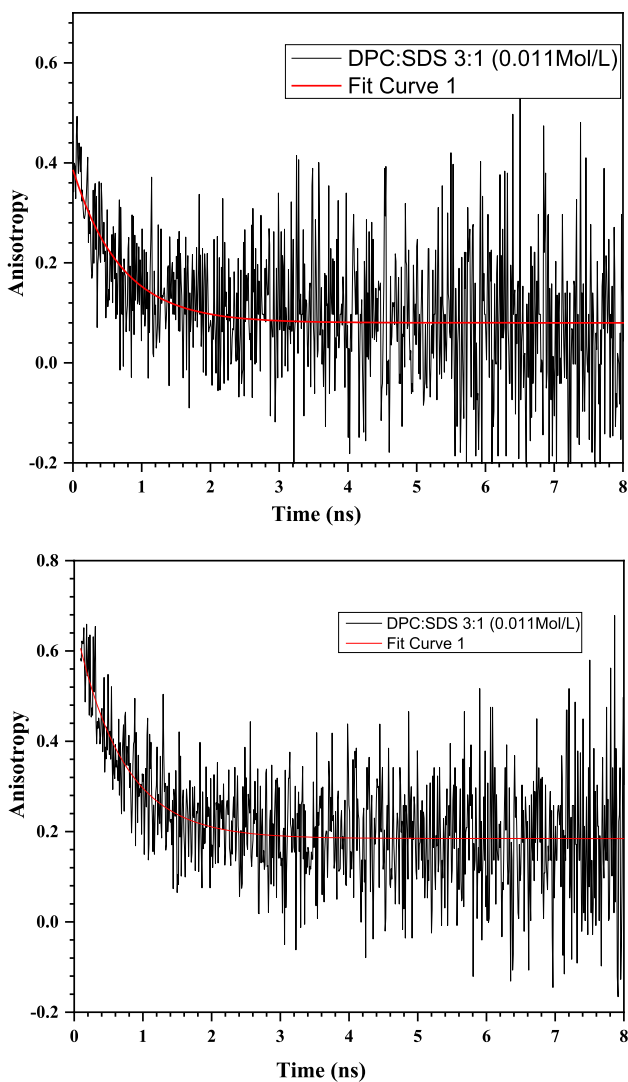


Fig. 5 The time decay anisotropy of both CMCs and the tail fitting according to the pierren model $(r(t) = (r_0 - r_\infty) \exp(-t/\tau_c) + r_\infty)$

volume (V) of the diffused molecules depending on the viscosity of the medium (η) and the temperature in kelvin:

$$\tau_c = \frac{\eta V}{kT},$$

where k is the Boltzmann constant.

from the previous relation, the average volume of micelles can be measured for both concentrations as it is presented in Table 2. The average volume varied slightly for both concentrations, hence we can conclude that the monomers have succeeded to perform self-assembly forming the micelles.

The FTIR spectra of SDS, DPC, SDS_{CMC}, DPC-SDS_{CMC}, and SDS_{CMC} are displayed in Fig. 6. The FTIR spectrum bands for SDS revealed distinct peaks at the 3291 cm⁻¹ (–OH stretching), 2900, 2841, and 1281 cm⁻¹

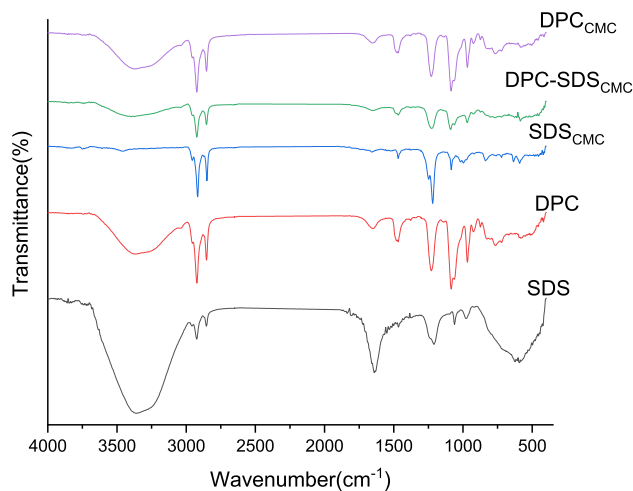


Fig. 6 FTIR spectrum of various concentrations of a DPC, 3:1 DPC/SDS, and SDS

(–CH₂ stretching and bending modes), the 1208 cm⁻¹ (S–O stretch), the 1027 cm⁻¹ (C–C band stretching), and the 800 and 400 cm⁻¹ (asymmetric C–H bending of the CH₂ group) [27]. FTIR spectrum bands for DPC revealed discrete peaks at 2900, 2841 cm⁻¹ (–CH₂ stretching and bending modes, and 1072–487 cm⁻¹ (P–O) [28]. The formation of the DPC, SDS micelle can be confirmed by FTIR spectroscopy comparing the spectrum of the micelle with the individual components (N-dodecyl phosphocholine and sodium dodecyl sulfate) as seen in Fig. 6. There was a significant difference between the SDS_{CMC}, DPC-SDS_{CMC}, SDS_{CMC} and SDS, DPC. The spectrum also displayed a diminished intensity in the peak at 1642 cm⁻¹. These results suggested that hydrogen bonding between N-dodecyl phosphocholine and sodium dodecyl sulfate plays a foremost role during the formation of the micelle. These data suggested that hydrogen bonding might present itself throughout the formation of the micelle because the intensity of the vibration bands of the methylene group concerned with interaction changed and some diminished.

Gibb's free energy of micellization is produced from the surfactant's critical micelle concentration (CMC), the Gibbs free energy of micellization can be approximated as:

$$\Delta G_{micellization} = RT \ln(CMC) \quad [30]$$

where ΔG_{mic} Is the change in Gibbs free energy of micellization, RT is the thermal energy, CMC is the critical micelle concentration.

The enthalpy of micellization (ΔH_{mic}) are evaluated the CMCs are first correlated by a polynomial equation, (ΔH_{mic}) is obtained based on the following thermodynamic relation:

$$\Delta H_{\text{mic}} = RT^2 \frac{d \ln CMC}{dT}$$

The entropy of micellization ΔS_{mic} is obtained from the relationship:

$$\Delta G_{\text{mic}} = \Delta H_{\text{mic}} - T\Delta S_{\text{mic}} \quad [7]$$

ΔG_{mic} is Gibbs free energy, ΔH_{mic} is the enthalpy of the system, T is temperature, ΔS_{mic} is the entropy of the system.

Gibb's free energy of micellization is produced from the surfactant's critical micelle concentration (CMC). Thermodynamic parameters obtained from micelle formation are listed in Table 3 for DPC, SDS, and DPC/SDS mixed [30].

The thermodynamic parameters were graphed versus temperature. Figure 7 depicts the temperature-dependent variation of these surfactants' thermodynamic parameters. Table 3 also shows that the ΔG_{mic} is negative and decreases with increasing temperature in the entire studied temperature range. The ΔG_{mic} negative value is similar to the previous

studies. [7, 31, 32]. Micellization is exothermic for the studied surfactants in the temperature range (ΔG_{mic} is negative). ΔS_{mic} appears to increase with temperature; the increase in ΔS_{mic} in a solution can be explained by the fact that, in the unassociated form, the surfactant molecules are free to ramble around in the aqueous medium. But in the form of a micelle, they get agglomerated that decreasing the independent movement freedom (decreasing the entropy of the system). The water molecules form an iceberg around the molecules of the surfactant resulting in an overall ordering of the system, translocating the surfactant molecules from the aqueous medium to the micelle core would break the iceberg that in turn positively elevate the entropy of the system. Furthermore, the rotational freedom degree of the surfactant hydrophobic chain in the nonpolar micelle core is considerably greater than in the aqueous medium; the entropy of micellization is negative in all temperature ranges and increases with temperature (the micellization process is exothermic). It can be explained that as temperature rises,

Table 3 Variation of the thermodynamic parameters of micelle formation for the DPC, b 5:1 c DPC/SDS, and d 3:1 DPC/SDS, e 1:1 DPC/SDS, f SDS as a function of temperature

Micelles	T (K)	ΔH_{mic} (KJ mol ⁻¹)	ΔG_{mic} (KJ mol ⁻¹)	$T\Delta S_{\text{mic}}$ (KJ mol ⁻¹)
DPC	288	1.599	-8.823	-10.422
	298	0.893	-9.190	-10.082
	308	0.078	-9.498	-9.576
	318	-0.849	-9.774	-8.925
	328	-1.896	-10.059	-8.163
	338	-3.068	-10.355	-7.287
5:1 DPC/SDS	288	4.780	-9.096	-13.876
	298	2.559	-9.583	-12.142
	308	0.0002	-10.082	-10.083
	318	-2.914	-10.103	-7.189
	328	-6.200	-10.359	-4.159
	338	-9.876	-10.423	-0.547
3:1DPC/SDS	288	6.840	-10.590	-17.430
	298	3.210	-11.129	-14.339
	308	-0.964	-11.549	-10.585
	318	-5.711	-11.628	-5.917
	328	-11.058	-11.928	-0.870
	338	-17.033	-12.292	4.741
1:1DPC/SDS	288	11.786	-8.823	-20.609
	298	6.763	-9.467	-16.231
	308	0.969	-9.905	-10.874
	318	-5.635	-10.043	-4.408
	328	-13.089	-10.182	2.907
	338	-21.432	-10.423	11.009
SDS	288	0.391	-9.646	-10.037
	298	-0.819	-10.110	-9.2902
	308	-2.197	-10.259	-8.062
	318	-3.752	-10.410	-6.658
	328	-5.491	-10.682	-5.191
	338	-7.424	-10.937	-3.514

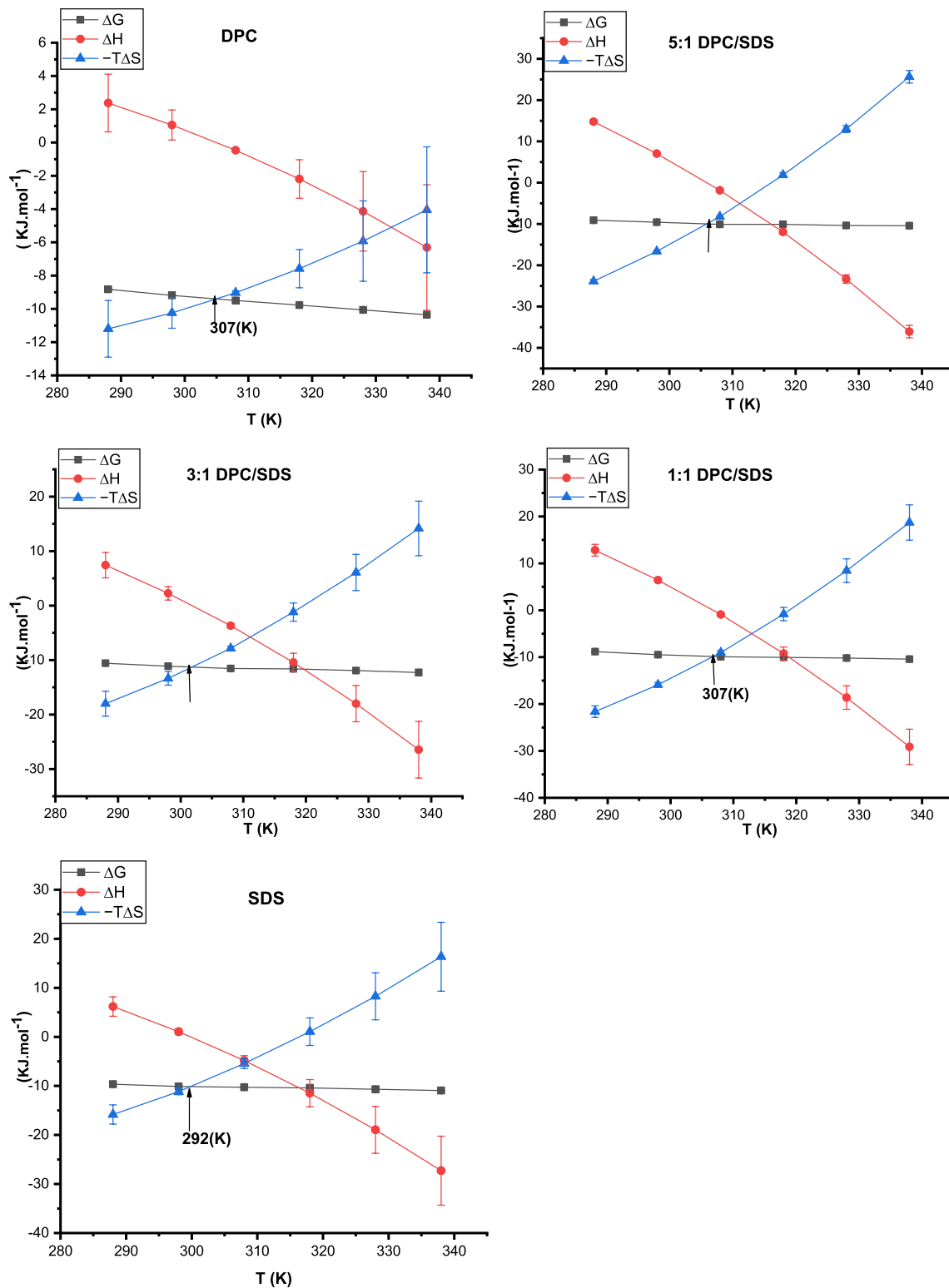


Fig. 7 Variation of the thermodynamic parameters for the micelle formation for the DPC, b 5:1 c DPC/SDS, and d 3:1 DPC/SDS, e 1:1 DPC/SDS, f SDS versus temperature. The intersection of the second

polynomial equation of ΔG_{mic} and $-T\Delta S_{\text{mic}}$ as a function of temperature is the transition temperature, T_0

the head group becomes more hydrated than the hydrophobic tail, increasing the order of the system and a decrease in entropy.

The temperature (T_0) at which the enthalpy of micellization equals zero and the process becomes entropically driven is calculated by intersecting the second polynomial approximation of the temperature dependence of ΔG_{mic} and $-T\Delta S_{\text{mic}}$ terms, as shown in Fig. 7. T_0 temperatures were determined to be 307, 306, 304, 308, 292 K for DPC, 5:1 DPC/SDS, 3:1 DPC/SDS, 1:1 DPC/SDS, and SDS, respectively. T_0 lower as the concentration of negatively charged DPC is high as in 5:1 DPC/SDS, and 3:1 DPC/SDS.

3.2 Micellization heat capacity

At constant pressure, the first derivatization of ΔH_{mic} gives heat capacity ΔC_{mic} . As the equation of enthalpy is linear in the studied temperature range. The dry hydrogen atoms number (n_{H}) in a surfactant micelle with a straight hydrocarbon chain that is not in contact with water is represented by this corresponding equation:

$$\Delta C_{\text{mic}} = 33n_{\text{H}} \quad [34].$$

In the current study, all of the ΔC_{mic} values were negative in all entire temperature ranges studied, leading to micelle formation. ΔC_{mic} values become more negative as the temperature rises.

ΔC_{mic} values at 338 K are -93.228 , -292.784 , -476.895 , -663.580 , and $-156.121 \text{ J mol}^{-1} \text{ K}^{-1}$ a DPC, b 5:1 c DPC/SDS, d 3:1 DPC/SDS, e 1:1 DPC/SDS, and f SDS, respectively. It is found that about 3, 8, 14, 20, and 5 hydrogen atoms are not in contact with water in DPC, SDS, 9:1 DPC/SDS, and 5:1 DPC/SDS, respectively, corresponding to the terminal methyl group for DPC micelle, two methylene groups for pure SDS, and three, six, and eight methylene groups for 5:1 DPC/SDS, 3:1 DPC/SDS, 1:1 DPC/SDS. From these results, we can conclude that the DPC/SDS mixed micelles appear to be less exposed to hydrophobic tails to water than the pure surfactants, which could indicate a more compact assembly and a higher aggregation number.

ΔH_{mic} can be supposed to show the change in hydrophobic dehydration during micellization. The greatest changes in ΔH_{mic} are observed for 1:1 DPC/SDS, where hydrophilic dehydration is associated with a sodium ion, sulphate polar headgroup, and phosphate group as well as hydrophobic dehydration.

3.3 Enthalpy–entropy compensation

The free energy ΔG_{mic} is estimated to be negative for all temperature ranges in Table 3, which means the micelle formation process is thermodynamically favorable. At lower

temperatures, the entropy contribution to the free Gibbs energy is significant compared to the enthalpy term. At higher temperatures, the ΔH_{mic} becomes more negative, and its contribution to the ΔG_{mic} increases. However, the entropy of micellization is calculated to be positive and decreased at higher temperatures. As a result its contribution to the ΔG_{mic} also decreases. Thus, ΔG_{mic} reveals a slight temperature dependence. Differences in the standard enthalpy of reaction ΔH_{mic} for different reactions may be compensated for by differences in the standard entropy of reaction ΔS_{mic} . Figure 8 the enthalpy–entropy compensation results.

Enthalpy–entropy compensation is the concept of the linear relationship between either the enthalpies ΔH_{mic} and entropies of activation ΔS_{mic} changes of a series of similar reactions, implies the following equation:

$$\Delta H_{\text{mic}} = T_c \Delta S_{\text{mic}} + \Delta H_{\text{mic}}^* \quad [35, 36]$$

in which T_c (The slope) is the compensation temperature, ΔH_{mic}^* (the intercept) characterizes the solute–solute interactions corresponding to the entropy change at a specific temperature giving ΔH_{mic}^* (degrees)=0, at which the driving force of micelle formation comes only from the entropy term; this temperature is characteristic of the surfactant species. The enthalpy–entropy compensation graphed for the micelles studied are in Fig. 8.

The T_c values are 317.34 K, 313.59 K, 318.57 K, 317.83 K, and 315.16 K for the DPC, 5:1 DPC/SDS, 3:1 DPC/SDS, 1:1 DPC/SDS, and SDS respectively, and are similar with those in previous studies for different surfactants [7]. The higher T_c value found for the 3:1 DPC/SDS mixed micelle than for the other surfactants could be due to some variance in the water–surfactant interaction through the micelle formation. The ΔH_{mic}^* values are -9.829 , -10.229 , -12.096 , 10.525 , and $-10.535 \text{ kJ mol}^{-1}$.

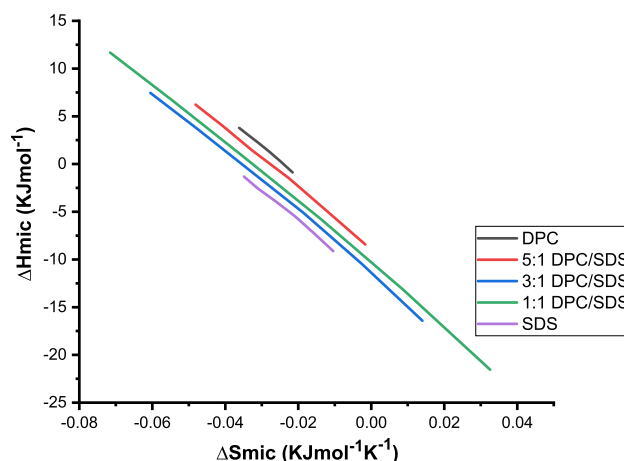


Fig. 8 Enthalpy–entropy compensation graph for the DPC, b 5:1 c DPC/SDS, and d 3:1 DPC/SDS, e 1:1 DPC/SDS, f SDS

The variation between DPC, 5:1 DPC/SDS, 3:1 DPC/SDS, 1:1 DPC/SDS, and SDS is small in this case, supporting the theory that with a fixed number of carbon atoms in a straight hydrocarbon tail, surfactants with different polar head groups display a minor difference in the intercept ΔH_{mic}^* . The chemical bond formation in the activation process often has negative effects on both ΔH_{mic}^* and ΔS_{mic}^* , [36]. The slight drop in ΔH_{mic}^* caused by the addition of SDS to DPC, on the other hand, can be accounted for by the increased stability of the zwitterionic micelles. We may conclude that when SDS/DPC mixed micelles are formed, the hydrophobicity of the micellar core increases while repulsive forces between SDS anionic heads diminish. These factors improve the stability of micellar systems.

4 Conclusion

The micelle formation of cationic DPC and anionic SDS in an aqueous media has been studied by the fluorometric method across the entire temperature range of (288–338)°K. The temperature dependence of the CMC and the micellization process have been investigated for DPC, SDS, and mixed micelles. The CMC firstly decreases and then increases. The minimum CMC is for 3:1 DPC/SDS (0.0110) mM occurred at 308 K. ΔH_{mic} was positive, indicating that at a lower temperature the micelle formation process was endothermic and becomes increasingly exothermic as the temperature increases $T > 308$ K. It is discovered that ΔG_{mic} decreased as temperature increases. addition of DPC to SDS in a small portion increases the hydrophobicity of the micellar core and decreases repulsive forces between SDS anionic heads. The lowest ΔH_{mic}^* observed in 3:1 DPC/SDS refers to enhancement in these interactions. We may conclude that DPC/SDS mixed micelle is more stable than pure ones.

Funding Open access funding provided by The Science, Technology & Innovation Funding Authority (STDF) in cooperation with The Egyptian Knowledge Bank (EKB). The study was funded by Science and Technology Development Fund (STDF).

Availability of data and materials All data, models, and code generated or used during the study appear in the submitted article.

Open Access This article is licensed under a Creative Commons Attribution 4.0 International License, which permits use, sharing, adaptation, distribution and reproduction in any medium or format, as long as you give appropriate credit to the original author(s) and the source, provide a link to the Creative Commons licence, and indicate if changes were made. The images or other third party material in this article are included in the article's Creative Commons licence, unless indicated otherwise in a credit line to the material. If material is not included in the article's Creative Commons licence and your intended use is not permitted by statutory regulation or exceeds the permitted use, you will need to obtain permission directly from the copyright holder. To view a copy of this licence, visit <http://creativecommons.org/licenses/by/4.0/>.

References

1. S. Kim et al., Overcoming the barriers in micellar drug delivery: loading efficiency, in vivo stability, and micelle–cell interaction. *Expert Opin. Drug Deliv.* **7**(1), 49–62 (2010)
2. M.J. Hajipour et al., Personalized disease-specific protein corona influences the therapeutic impact of graphene oxide. *Nanoscale* **7**(19), 8978–8994 (2015)
3. M. Chamundeeswari, J. Jeslin, M.L. Verma, Nanocarriers for drug delivery applications. *Environ. Chem. Lett.* **17**(2), 849–865 (2019)
4. O. Akhavan, E. Ghaderi, Graphene nanomesh promises extremely efficient in vivo photothermal therapy. *Small* **9**(21), 3593–3601 (2013)
5. L. Wang et al., Therapeutic peptides: current applications and future directions. *Signal Transduct. Target. Ther.* **7**(1), 48 (2022)
6. N. Rabiee et al., CaZnO-based nanohosts for the detection of ssDNA, pCRISPR and recombinant SARS-CoV-2 spike antigen and targeted delivery of doxorubicin. *Chemosphere* **306**, 135578 (2022)
7. E. Sikorska et al., Thermodynamics, size, and dynamics of zwitterionic dodecylphosphocholine and anionic sodium dodecyl sulfate mixed micelles. *J. Therm. Anal. Calorim.* **123**(1), 511–523 (2016)
8. N. Scholz, T. Behnke, U. Resch-Genger, Determination of the critical micelle concentration of neutral and ionic surfactants with fluorometry, conductometry, and surface tension—a method comparison. *J. Fluoresc.* **28**(1), 465–476 (2018)
9. T. Chakraborty, I. Chakraborty, S. Ghosh, The methods of determination of critical micellar concentrations of the amphiphilic systems in aqueous medium. *Arab. J. Chem.* **4**(3), 265–270 (2011)
10. Turro, N.J., et al., *Principles of molecular photochemistry: an introduction* (University science books, 2009)
11. W. Caetano, M. Tabak, Interaction of chlorpromazine and trifluoperazine with anionic sodium dodecyl sulfate (SDS) micelles: electronic absorption and fluorescence studies. *J. Colloid Interface Sci.* **225**(1), 69–81 (2000)
12. A. Domínguez et al., Determination of critical micelle concentration of some surfactants by three techniques. *J. Chem. Educ.* **74**(10), 1227 (1997)
13. Q. Zhu et al., A sensitive and visible fluorescence-turn-on probe for the CMC determination of ionic surfactants. *Chem. Commun.* **50**(9), 1107–1109 (2013)
14. G.K. Bains et al., The extent of pyrene excimer fluorescence emission is a reflector of distance and flexibility: analysis of the segment linking the LDL receptor-binding and tetramerization domains of apolipoprotein E3. *Biochemistry* **51**(31), 6207–6219 (2012)
15. L. Piñeiro, M. Novo, W. Al-Soufi, Fluorescence emission of pyrene in surfactant solutions. *Adv. Coll. Interface. Sci.* **215**, 1–12 (2015)
16. H. Li et al., Influence factors on the critical micelle concentration determination using pyrene as a probe and a simple method of preparing samples. *Royal Society open science* **7**(3), 192092 (2020)
17. H. Akbaş, Ç. Batıgöç, Micellization of dodecylpyridinium chloride in water-ethanol solutions. *Colloid J.* **70**(2), 127–133 (2008)
18. K.E. Ramohlola et al., Instrumental techniques for characterization of molybdenum disulphide nanostructures. *J. Anal. Methods Chem* **2020**, 8896698 (2020)
19. G. Bains, A.B. Patel, V. Narayanaswami, Pyrene: a probe to study protein conformation and conformational changes. *Molecules* **16**(9), 7909–7935 (2011)
20. S.S. Shah, A.M. Khan, Determination of critical micelle concentration (Cmc) of sodium dodecyl sulfate (SDS) and the effect of

- low concentration of pyrene on its Cmc using ORIGIN software. *J. Chem. Soc. Pakistan* **30**(6), 186 (2011)
21. T.J. Prazeres et al., Determination of the critical micelle concentration of surfactants and amphiphilic block copolymers using coumarin 153. *Inorg. Chim. Acta* **381**, 181–187 (2012)
 22. I. Garcia-Mateos, M. Mercedes Velazquez, L.J. Rodriguez, Critical micelle concentration determination in binary mixtures of ionic surfactants by deconvolution of conductivity/concentration curves. *Langmuir* **6**(6), 1078–1083 (1990)
 23. M. Prasad, S. Moulik, R. Palepu, Self-aggregation of binary mixtures of alkyltriphenylphosphonium bromides: a critical assessment in favor of more than one kind of micelle formation. *J. Colloid Interface Sci.* **284**(2), 658–666 (2005)
 24. Y. Xu et al., Vibrational band-structures caused by internal rotations of the boron Wankel rotor B 11-. *RSC Adv.* **11**(6), 3613–3621 (2021)
 25. S. Joshi, D.D. Pant, Steady state and time-resolved fluorescence spectroscopy of quinine sulfate dication bound to sodium dodecylsulfate micelles: fluorescent complex formation. *J. Lumin.* **145**, 224–231 (2014)
 26. J.L. Atwood, *Comprehensive Supramolecular Chemistry II* (Elsevier, Amsterdam, 2017)
 27. M. Hafizah, A. Riyadi, A. Manaf, Particle size reduction of polyaniline assisted by anionic emulsifier of sodium dodecyl sulphate (SDS) through emulsion polymerization. In *IOP Conference Series: Materials Science and Engineering*. 2019. IOP Publishing
 28. T. Fornaro et al., Hydrogen-bonding effects on infrared spectra from anharmonic computations: uracil–water complexes and uracil dimers. *J. Phys. Chem. A* **119**(18), 4224–4236 (2015)
 29. H. Butt, K. Graf, M. Kappl, *Physics and Chemistry of Interfaces Wiley* (Wiley, Weinheim, 2006)
 30. T. Heimburg, *Thermal Biophysics of Membranes* (Wiley-VCH, Berlin, 2007)
 31. M.E. Mahmood, D.A. Al-Koofee, Effect of temperature changes on critical micelle concentration for tween series surfactant. *Global J. Sci. Front. Res. Chem.* **13**(4), 1–7 (2013)
 32. E. Mohajeri, G.D. Noudeh, Effect of temperature on the critical micelle concentration and micellization thermodynamic of non-ionic surfactants: polyoxyethylene sorbitan fatty acid esters. *E-J. Chem.* **9**(4), 2268–2274 (2012)
 33. S. Gill, I. Wadsö, An equation of state describing hydrophobic interactions. *Proc. Natl. Acad. Sci.* **73**(9), 2955–2958 (1976)
 34. O. Exner, How to get wrong results from good experimental data: a survey of incorrect applications of regression. *J. Phys. Org. Chem.* **10**(11), 797–813 (1997)
 35. S. Khrapunov, The enthalpy-entropy compensation phenomenon. Limitations for the use of some basic thermodynamic equations. *Curr. Protein Peptide Sci.* **19**(11), 1088–1091 (2018)
 36. A. Cornish-Bowden, Entropy-enthalpy compensation, in *Encyclopedia of Biophysics*. ed. by G. Roberts, A. Watts (Springer, Berlin, 2018), pp.1–6

Publisher's Note Springer Nature remains neutral with regard to jurisdictional claims in published maps and institutional affiliations.